https://doi.org/10.5194/egusphere-2026-6373
Preprint. Discussion started: 19 November 2026
© Author(s) 2026. CC BY 4.0 License.

Changes in erosion rate, alluvial cover and roughness in a mixed alluvial-bedrock channel with downstream alternations in bedrock strength

Kazuaki Mutsuura[1], Takuya Inoue[1,2], Rebecca Hodge[3], and Tamaki Sumner[1], and Tatsuhiko Uchida[1]

[1] Graduate School of Advanced Science and Engineering, Hiroshima University, Hiroshima, Japan.
[2] Graduate School of Science and Technology, Gunma University, Gunma,Japan
[3] Department of Geography, Durham University, Durham, UK

Correspondence to: Takuya Inoue (inouetakuya@gunma-u.ac.jp)

Abstract. In a riverbed comprised of both hard and soft bedrock, soft bedrock with low erosion resistance would be expected to abrade faster than hard bedrock. However, it remains unknown how the relative strength of hard and soft bedrock, and the additional influence of sediment cover, will affect erosion rates. To address this gap, we conducted flume experiments simulating bedrock with alternating strength in the downstream direction and constant sediment supply. The difference in elevation between hard and soft bedrock approached a constant value over time. When soft bedrock eroded faster, the overlying sediment cover increased because of gravity and increased hydraulic resistance, decreasing erosion rates. We also compared across three runs with constant soft bedrock strength but varying hard bedrock strength. The soft bedrock erosion rate changed between the runs, demonstrating that the bedrock erosion rate is influenced not only by the strength at that specific location but also by the strength of the surrounding bedrock.

1 Introduction

The erosion rate of bedrock rivers depends on the balance between erosion of the bed by bedload, and protection of the bed by alluvial cover (Gilbert 1877, Sklar and Dietrich, 1998). However, bedrock erosion can alter the bed topography, affecting local hydraulics and hence sediment transport, and also the storage capacity of the bed for sediment cover (Hodge and Hoey 2016). These relationships are further complicated when the bedrock is heterogeneous, with spatial variations in strength, as bedrock erosion rate depends on the negative square of the bedrock tensile strength (Sklar and Dietrich, 2004; Auel et al.,2015 ; Inoue et al., 2017). Spatial variations in strength can result in difference in erosion rate, affecting the bed slope and surface roughness (Goode and Wohl, 2010), which in turn change the sediment transport and the alluvial cover, further altering the bedrock erosion rate (Mishra and Inoue. 2020; Chatanantavet and Parker, 2008; Roberto et al.,2019). That is, bedrock channel morphology reflects feedbacks between bedrock resistance and hydrodynamically driven forces, and sediment dynamics (Wohl and Merritt, 2001; Baynes et al., 2020).

https://doi.org/10.5194/egusphere-2026-6373
Preprint. Discussion started: 19 November 2026
© Author(s) 2026. CC BY 4.0 License.

The alluvial cover extent is a crucial parameter for estimating bedrock erosion rates, and many studies have been conducted on this topic. Sklar and Dietrich (2004) proposed a model in which the cover fraction P_c is a linear function of the ratio of sediment transport rate q_b to sediment transport capacity q_{bc}. In contrast, Turowski et al. (2007) proposed a model that considers the cover effect as an exponential function of q_b/q_{bc}. Chatanantavet and Parker (2008) conducted experiments in straight concrete channels with varying bedrock roughness to investigate the relationship between sediment supply and cover fraction. Their findings revealed that when bedrock roughness was high, the cover fraction increased linearly with sediment supply. In contrast, with low bedrock roughness, the transition from fully exposed to fully covered bedrock occurred abruptly as sediment supply increased. A similar pattern of rapid alluviation was observed in laboratory experiments conducted by Hodge and Hoey (2016a, b) using 3D-printed channels modeled after Trout Beck, a river in the North Pennines, UK. These results highlight the critical role of bedrock roughness in determining the cover fraction.

To account for the influence of bedrock roughness, Inoue et al. (2014) and Johnson (2014) independently proposed the macro-roughness model and surface roughness model, respectively. Both models theoretically demonstrated that in smooth bedrock rivers, P_c does not behave as a single-valued function of q_b/q_{bc}, but instead exhibits hysteresis. A detailed comparison of these models is provided in the review by Mishra and Inoue (2020). Focusing on numerical models that can predict spatial variations in alluvial cover, Hodge and Hoey (2012) developed a reach-scale cellular automaton model by assigning entrainment probabilities to individual particles. Their analysis indicated that rapid alluviation occurs only when particles in sediment patches are less mobile than isolated particles. Additionally, they proposed a sigmoid relationship between q_b/q_{bc} and $1-P_c$.

Aubert et al. (2016) proposed a discrete element model to determine the alluvial cover fraction P_c based on the velocity distribution of particles. In their model, particles settle as cover on the bedrock surface if their velocity is less than one-tenth of the maximum velocity. However, this model is unable to handle non-uniform velocity fields, meaning it cannot predict changes in the alluvial cover. Zhang et al. (2015) and Shobe et al. (2017) proposed the MRSAA and SPACE 1.0 models, which predict the simultaneous evolution of alluvial layers and bedrock. These models satisfy sediment mass conservation and can predict both the thickness of the alluvial cover and the depth of bedrock erosion. However, they do not account for the influence of bedrock roughness. Inoue et al. (2016, 2021) integrated a two-dimensional flow analysis model with the model by Inoue et al. (2014), creating the first model capable of analyzing the spatial effects of variations in bedrock roughness, water depth, and flow velocity on alluvial cover and bedrock erosion. Subsequently, Cho and Nelson (2024a, b) incorporated the impact of alluvial bedforms that develop on bedrock, which alter roughness, successfully reproducing the experiments of Chatanantavet and Parker (2008) with high accuracy.

Previous research has made significant progress in experiments, theoretical models, and numerical simulations of alluvial cover over bedrock. However, one important phenomenon remains largely unaddressed: the impact of spatial variations in bedrock strength on erosion rates, bed roughness and sediment cover formation, and how these interactions develop over time. When bedrock strength varies spatially (Fig. 1), steps between hard and soft bedrock are expected to form due to differences in erosion rates. If the erosion rate of soft bedrock remains greater than that of hard bedrock, the steps should become larger

https://doi.org/10.5194/egusphere-2026-6373
Preprint. Discussion started: 19 November 2026
© Author(s) 2026. CC BY 4.0 License.

over time. However, interactions between flow, sediment transport and topography may act to limit these effects. As the steps become larger, alluvial cover on soft bedrock may increase through the effects of gravitational deposition into low-lying soft bedrock, increasing protection of these areas. The changing bed topography could also affect flow hydraulics, with steps potentially shielding low-lying areas, and reducing flow velocity, which may further decrease soft bedrock erosion rates. This raises the question of whether an equilibrium exists where the erosion rates of hard and soft bedrock are equal. To address this gap, this study conducts laboratory experiments using riverbeds with alternating soft and hard bedrock layers along the flow direction (e.g., Fig. 1b) to investigate the changes in sediment cover, bedrock roughness and bedrock erosion.



Figure 1: Example of a bedrock river with alternating soft and hard sand soil layers (Toyohira River, Hokkaido, Japan) & Experimental flume. In the flume the red riverbed is colored low-strength concrete, and strength alternates longitudinally.

https://doi.org/10.5194/egusphere-2026-6373
Preprint. Discussion started: 19 November 2026
© Author(s) 2026. CC BY 4.0 License.

2 Methods

We used a 3 m long, 0.1 m wide rectangular channel, with slope of 0.0077 and a weak concrete bed as a bedrock simulant (e.g., Inoue et al., 2023, 2024). The concrete had alternating soft and hard sections spaced 80 mm apart in the streamwise direction (Fig. 1). Three runs were performed in which the soft bedrock strength, flow discharge, sediment supply rate and supplied sediment grain size were kept constant and only the hard bedrock strength was varied. The soft bedrock cement mix ratio was 1:150:24.8 (Portland cement: 0.34 mm diameter silica sand: water), and its unconfined compressive strength measured using a simple needle penetration test (SH-70, MARUTO Testing Machine Company), was 5.40±0.78 kPa. The cement mix ratios of hard bedrock were 1:100:16.5 for Run 1, 1:40:6.6 for Run 2, and 1:20:3.3 for Run 3, with compressive strengths of 18.26±0.58 kPa for Run 1, 27.86±0.56 kPa for Run 2, and 97.47±1.31 kPa for Run 3 (± standard error for five strength tests). We observed that the concrete only erodes via particle-impact abrasion, and not by water alone. 0.5 m sections near the upstream and downstream ends of the channel were fixed beds to prevent a knickpoint forming and migrating from the downstream end. Flow discharge and sediment supply rate were kept constant at 11.9 g/s and 2.1 g/s respectively. The supplied sediment was well-sorted rounded silica sand with an average grain size of 1.2 mm. Each experimental run was 7 hours long. We stopped the pump every hour and took vertical photographs to measure the bed area covered by the sediment. Sediment was removed with a vacuum cleaner, and the bedrock erosion depth was measured with a 3D scanner (Artec Leo, a 3D resolution up to 0.2 mm, a 3D point accuracy of 0.1 mm). The measurement section was 0.8 m long, i.e. five hard/soft pairs, located 1.14 m to 1.94 m from the upstream end. The point cloud was gridded into a DEM with a resolution of 0.5 mm. To quantify bedrock surface roughness, we calculated the areal and longitudinal standard deviations (σ_a, σ_l) from the DEM:

$$\sigma_a = \sqrt{\frac{1}{ni \times nj} \sum_{i,j=1}^{ni,nj} \left(Z_{i,j} - Z_{ave}\right)^2} \quad (1)$$

$$\sigma_l = \frac{1}{nj} \sum_{j=1}^{nj} \sqrt{\frac{1}{ni} \sum_{i=1}^{ni} \left(Z_{i,j} - Z_{ave,j}\right)^2} \quad (2)$$

here, i,j are the grid number in longitudinal and transverse directions, respectively, ni,nj are the maximum grid number in longitudinal and transverse directions, respectively, $Z_{i,j}$ is the bedrock surface elevation, Z_{ave} is the averaged elevation in the area (i,j=1 ~ni,nj), $Z_{ave,j}$ is the averaged elevation in the longitudinal line (i=1 ~ni) when the grid number is j. The standard deviations were calculated for each 0.8 m × 0.1 m area of different strength, and the average values were calculated separately for hard and soft bedrock. Consequently standard deviations do not account for any differences in elevation between hard and soft bedrock areas.

We calculated the hydraulic roughness height k_s using the mean velocity formula based on the logarithmic velocity distribution as expressed in terms of the Keulegan equation:

https://doi.org/10.5194/egusphere-2026-6373
Preprint. Discussion started: 19 November 2026
© Author(s) 2026. CC BY 4.0 License.

$$\frac{U}{u_*} = 6.0 + 5.75\log_{10}\left(\frac{D}{k_s}\right) \quad (3)$$

where U is flow velocity (=Q/BD), u_* is shear velocity (=$\sqrt{gDI}$), Q is flow discharge, B is flume width, D is flow depth, g is gravitational acceleration, and I is water surface slope. Every hour we measured channel center flow depth using a point gauge at distances of 1.34 and 1.50 m (soft bedrock), and 1.42 and 1.58 m (hard bedrock) from the upstream end. Water surface slope was calculated based on water levels measured at 0.08 m intervals from images taken from the side of the flume and longitudinal distance along the flume. Although the water surface was locally wavy (Fig. 1), the averaged water surface slope of the measured section was constant throughout the experiment, at $7.7\text{x}10^{-3} \pm 6\text{x}10^{-7}$, which we use in Eq. (3).

3 Results

In Run 1 (smallest difference in bedrock strength), two longitudinal grooves formed, and the erosion depth in the center was smaller than in the areas closer to the banks (Figs. 2a and 3a). The difference in hard and soft bedrock average erosion depth was less than 0.79 mm. In contrast, in Run 2 and Run 3, with intermediate and large differences in bedrock strength, the erosion depth varied with bedrock strength, forming a topography with transverse steps (Figs. 2b c). The difference in average erosion depth between hard and soft bedrock was 2.77 mm in Run 2 and 2.62 mm in Run 3. Despite the soft bedrock being the same in all three runs, it eroded most in Run 2, suggesting that the soft bedrock erosion rate varies with the hard bedrock strength and/or the eroded bed topography.

In Run 1, the sediment was transported in two longitudinal stripes. Over time, bedrock was eroded along the transport paths forming longitudinal grooves in which alluvial cover developed. Almost no sediment was transported on the higher uneroded areas of the bed. In Run 2, alternate-bar-like alluvial cover developed early in the experiment. The areas of deposition migrated downstream similar to alternate bars in alluvial rivers. Bedrock was eroded in areas without alluvial cover or with thin alluvial layers. The soft bedrock erosion rate was 13.8 mm/420 min and faster than that of hard bedrock, so soft bedrock areas were preferentially lowered and alluvial cover increased in these areas. The same happened in in Run 3, but the alluvial cover extent in the hard bedrock areas was less than that in Run 2. It's interesting that the difference in bedrock strength between Run 1 and Run 2 is far smaller than between Run 2 and Run 3, but that Run 2 and Run 3 are the ones that behave the same way.

In Run 1 (small strength difference), there was more erosion than in Run 3, but there was little difference in the erosion depth between the hard and soft bedrock (Fig. 3a). The bedrock erosion rate was highest in 60 min to 120 min, and then decreased (Fig.3a). Despite the alluvial cover fraction only reaching 0.7-0.8 after 300 minutes (Fig. 3b), bedrock erosion did not progress after this time in the experiment. This is due to the formation of longitudinal grooves in which most sediment was concentrated with a cover fraction of one, with little sediment moving over the adjacent areas with a cover fraction of zero.

In Run 1, the bedrock surface standard deviation is higher than in Runs 2 and 3 (Fig. 3c). However, the hydraulic roughness height is the lowest among the three runs (Fig. 3e). One possible reason is that the standard deviation includes transverse roughness (i.e. the cross-stream difference in elevation between the grooves and ridges) which does not contribute to flow

https://doi.org/10.5194/egusphere-2026-6373
Preprint. Discussion started: 19 November 2026
© Author(s) 2026. CC BY 4.0 License.

resistance (i.e., hydraulic roughness height). In contrast, the longitudinal standard deviation only accounts for roughness in the flow direction. The Run 1 standard deviation is about three times that of Runs 2 and 3 (Fig. 3c), whereas the longitudinal standard deviation is only twice (Fig. 3d), but this still does not account for the observed differences in hydraulic roughness. Another possibility is that the bedrock standard deviation does not represent the bed topography during the experiment, as the bottom of the grooves were covered with sediment reducing the overall topographic roughness (Fig. 2a).

In Run 2 (medium strength difference), the bedrock erosion rate was highest in the first 60 min, and then decreased (Fig. 3a). The elevation difference between soft and hard bedrock increased until 180 min, and then remained similar. The cover fraction was maintained at 0.95-1 for the soft bedrock areas and 0.5-0.7 for the hard bedrock areas after 180 min (Fig. 3b).

Since soft bedrock erosion continued after 180 min, we infer that the alluvial cover over soft bedrock was not sufficiently thick to prevent erosion, with bedload particles still hitting the bedrock. Over time, the standard deviation and the hydraulic roughness height approached constant values (Figs. 3c, d and e). In Run 3 (largest strength difference), the erosion rate of both soft and hard bedrock was slower than in Run 2, but the time series of erosion depth shows a similar trend (Fig. 3a). The final difference in erosion depth between soft and hard bedrock was 2 to 2.5 mm, which is very similar to Run 2 (average value was 2.32 mm), despite the higher difference in strength between soft and hard bedrock (Fig. 3f). The alluvial cover fraction was maintained at 0.8-1 on the soft bedrock and 0.3-0.45 on the hard bedrock after 60 minutes (Fig. 3b). The similar elevation difference between the soft and hard bedrock in Runs 2 and 3 suggests that the slower erosion rate caused by the harder bedrock of Run 3 was compensated for by a smaller alluvial cover fraction. Furthermore, despite having the same strength, the erosion rates of the soft bedrock differ between Run 2 and Run 3, with values of 13.80 mm/420 min and 8.96 mm/420 min respectively. With the exception of the hard bedrock in Run 3, positive correlations are observed between bedrock surface standard deviation and alluvial cover fraction (Figs. 4a, b, c), suggesting that alluvial cover is mainly determined by surface irregularities at the grain-size scale. However, the hard bedrock standard deviation is larger in Run 3 is than Run 2, yet the hard bedrock cover fraction in Run 3 is smaller (Figs. 3a and b), suggesting that other factors e.g. form drag (flow turbulence) caused by bedrock steps and alluvial bars, also influence the alluvial cover. The standard deviation for the entire flume followed a similar trend to that of soft and hard bedrock in all cases. There is little correlation between standard deviation and hydraulic roughness (Fig. 4d) because bedrock standard deviation only describes bedrock topography within each bedrock section, and not form drag from bedrock steps, surface drag from alluvial deposits, and the form drag from bedforms such as bars.

There is a negative correlation between alluvial cover fraction and bedrock erosion rate (Fig. 4e). The erosion rate approaches 0 at an alluvial cover fraction of about 0.7 in Run 1, as explained previously. In contrast, in Runs 2 and 3, even when the alluvial cover fraction approaches 1, the erosion rate is not zero. This is because the alluvial layer is too thin to prevent erosion.

https://doi.org/10.5194/egusphere-2026-6373
Preprint. Discussion started: 19 November 2026
© Author(s) 2026. CC BY 4.0 License.

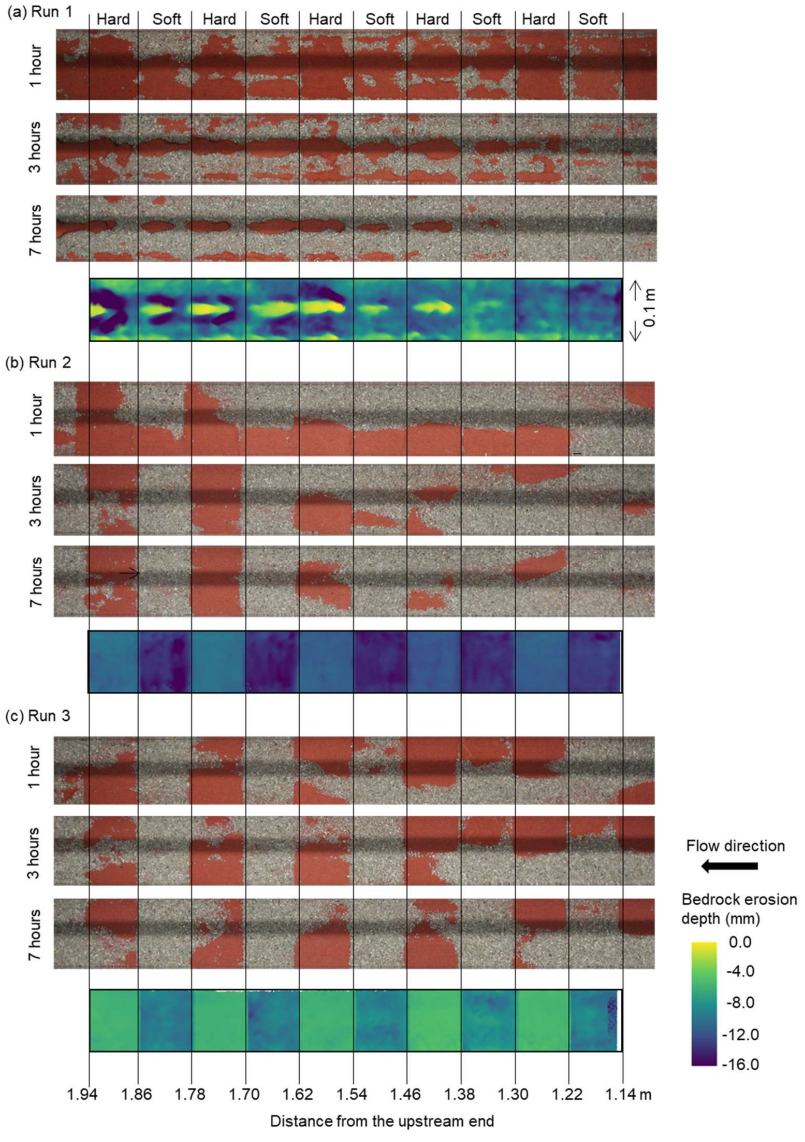


Figure 2: Vertical photographs of alluvial cover and color map of elevation change from initial bed and (a) Run 1 with the smallest difference in bedrock strengths, (b) Run 2 with intermediate difference, and (c) Run 3 with largest difference. The red area is bedrock and the white area is deposited sediment.

https://doi.org/10.5194/egusphere-2026-6373
Preprint. Discussion started: 19 November 2026
© Author(s) 2026. CC BY 4.0 License.

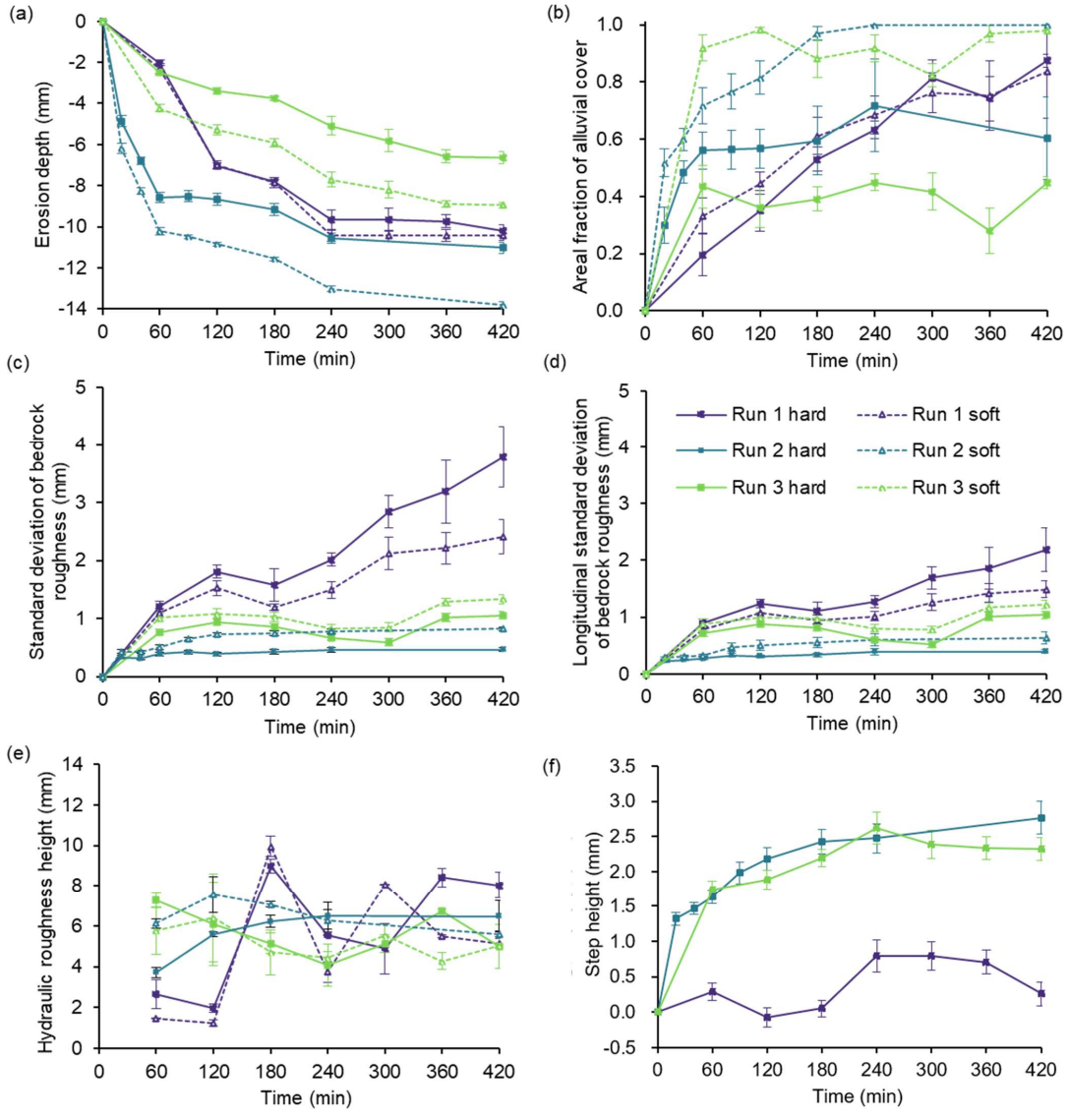


Figure 3: Time series of (a) changes in bedrock erosion depth, (b) areal fraction of alluvial cover, (c) standard deviation of bedrock surface, (d) standard deviation of bedrock surface in the longitudinal direction, (e) hydraulic roughness height, and (f) difference in erosion depth between soft and hard bedrock .

https://doi.org/10.5194/egusphere-2026-6373
Preprint. Discussion started: 19 November 2026
© Author(s) 2026. CC BY 4.0 License.

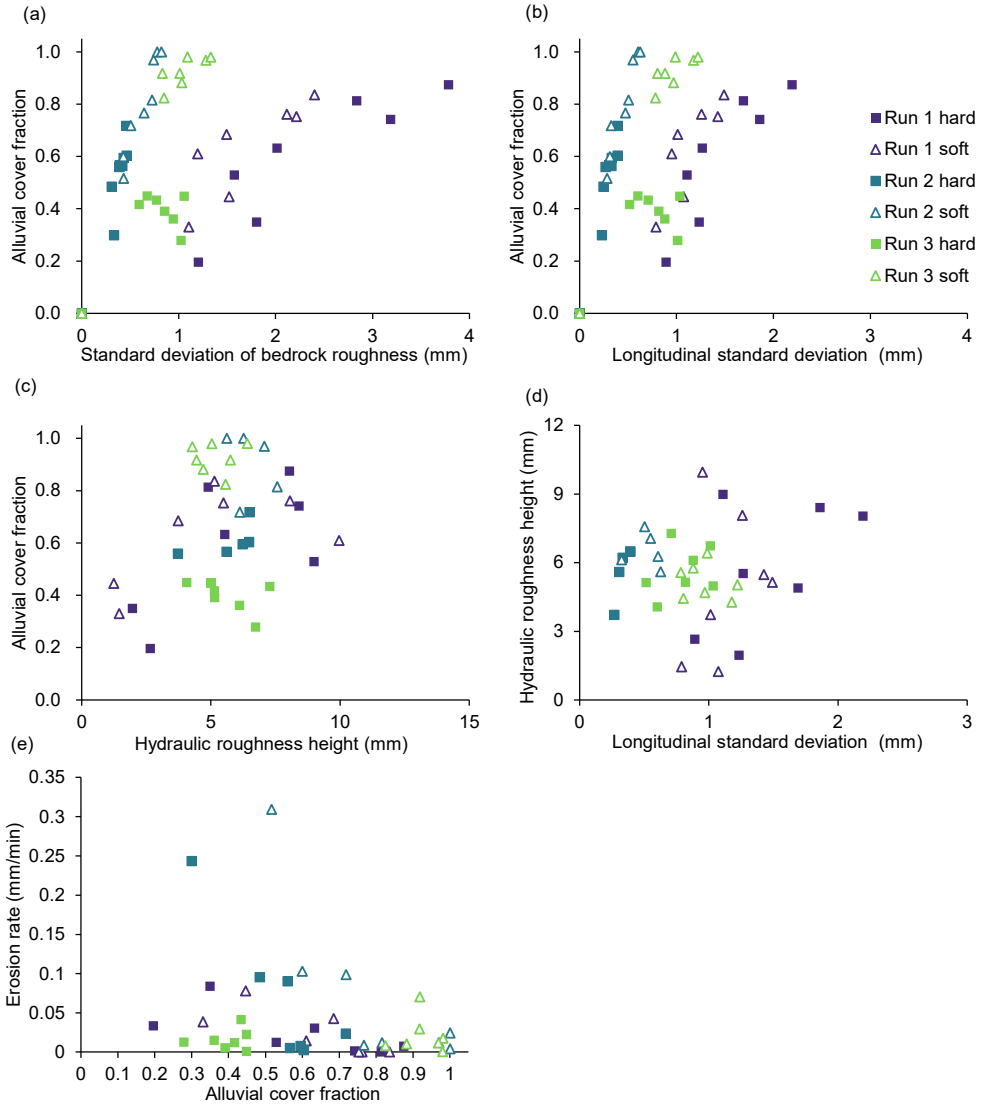


Figure 4: Relationship between (a) alluvial cover fraction and standard deviation of bedrock roughness, (b) alluvial cover fraction and standard deviation of bedrock roughness in longitudinal direction, (c) alluvial cover fraction and hydraulic roughness height, (d) hydraulic roughness height and standard deviation of bedrock roughness, and (e) bedrock erosion rate and alluvial cover fraction.

175

https://doi.org/10.5194/egusphere-2026-6373
Preprint. Discussion started: 19 November 2026
© Author(s) 2026. CC BY 4.0 License.

4 Discussion

4.1 Bed topography

One of the main differences between runs was the formation of longitudinal grooves in Run 1 and alternate bars and bedrock steps in Runs 2 and 3. In alluvial rivers, alluvial bars are predicted to form when the aspect ratio B/D is larger than the critical aspect ratio e.g., Kuroki and Kishi, 1984; Colombini et al., 1987). The critical ratio varies with grain size, gradient, and Shields number. In our experimental conditions (initial water depth D = 25 mm, channel width B = 0.1 m, shields number $\tau^* = 0.1$, grain size d = 1.2 mm, bed slope I = 0.0077), the critical value is approximately 16 to 17（Kuroki and Kishi, 1984; Colombini et al., 1987) and B/D is 4, so bars are not expected.

However, in bedrock rivers, theoretical analysis has shown that there may not be a critical value of aspect ratio required for bar formation (Nelson and Seminara, 2012). Experimental and numerical results have indicated that the ratio of sediment supply rate to transport capacity is more important than the aspect ratio in bedrock channels (Inoue et al., 2016; Inoue and Nelson, 2020). When the supply to capacity ratio is smaller than 0.5, longitudinal grooves form due to turbulence driven secondary flows (Inoue et al., 2016; Inoue and Nelson, 2020). When the supply to capacity ratio is 0.7 to 0.9, a mixture of bars and grooves occurs, and as the value approaches 1, bars form (Inoue et al., 2016; Inoue and Nelson, 2020). Conditions between 0.5 and 0.7 have not been tested. The results from this study are consistent with these predictions. All runs had the same initial aspect ratio (B/D=4) and supply to capacity ratio, but B/D values changed to 0.26 in Run 1, 0.64 in Run 2, and 0.68 in Run 3 after 1 hour. In Run 1, where there was little difference in erosion between soft and hard bedrock and hence low hydraulic roughness, the supply-to-capacity ratio was small, so grooves developed. The development of two grooves in Run 1 is consistent with half of the river width-to-depth ratio (Inoue et al.,2020). In Runs 2 and 3, where the strength difference was large and the roughness increased, the supply-to-capacity ratio also increased, and bars became dominant.

In a straight flume, the transition from nappe flow to skimming flow depends primarily on the discharge, step height, and channel slope. As demonstrated by Hubert (1994), when the critical flow depth-to-step height ratio exceeds a threshold value (e.g. depth-to-step height ratio exceeds $1.057 - 0.465(h/l)$) the flow glides over the step edges. The momentum transfer between the main stream and the closed recirculating vortices generates significant fluid shear, contributing significantly to rate-of-energy dissipation prior to the toe of the spillway. The critical flow depth-to-step height ratio were 30.8 to 477.9 (Run1), 9.9 to 18.5 (Run2), and 9.3 to 14.1 (Run3). As Run 1 exhibited a higher critical flow depth-to-step height ratio compared with other cases, and all cases exceeded a threshold value, this suggests that the flow was independent of the topography of the channel bed.

4.2 Bedrock erosion rate, alluvial cover and rock strength

Our experiments suggest that when the difference in rock strength exceeds a threshold, the steps formed at the boundary between hard and soft bedrock approach a constant height (Runs 2 and 3 in Fig. 3f), indicating that erosion rates of the hard

https://doi.org/10.5194/egusphere-2026-6373
Preprint. Discussion started: 19 November 2026
© Author(s) 2026. CC BY 4.0 License.

and soft bedrock are equal. In the models of Sklar and Dietrich (2004) and Inoue et al. (2017), bedrock erosion rate depends on the negative square of rock tensile strength (Sklar and Dietrich, 2004; Auel et al., 2015), the sediment supply rate, and the areal fraction of alluvial cover. In addition to above parameters, the model of Sklar and Dietrich (2004) includes Young's modulus and Shield's number and the model of Inoue et al. (2017) includes the ratio of grain size to bedrock roughness, but for simplicity we omit terms that are not common to both models. Equating the erosion rates of soft and hard bedrock leads to the following relationship,

$$E \propto {\sigma_{T,s}}^{-2} q_{bs}\left(1 - P_{c,s}\right) = {\sigma_{T,h}}^{-2} q_{bs}\left(1 - P_{c,h}\right) \quad (4)$$

where, E is the bedrock erosion rate, β is the abrasion coefficient, σ_T is the rock tensile strength, q_{bs} is the sediment supply rate, P_c is the areal fraction of alluvial cover, and the subscripts s and h denote soft and hard bedrock. Rearranging equation (4) gives

$$\frac{\left(1 - P_{c,h}\right)}{\left(1 - P_{c,s}\right)} \approx \left(\frac{\sigma_{T,h}}{\sigma_{T,s}}\right)^2 \quad (5)$$

i.e. when erosion rate is equal, the ratio of alluvial cover fraction between soft and hard bedrock depends on their strength ratio. In Run 2, the soft bedrock alluvial cover fraction $P_{c,s}$ at 7 hours is 1.0. Since P_c of 1.00 would produce zero bedrock erosion, we set it to 0.999. Substituting this value and the rock strengths in Run 2 into Eq. (5), $P_{c,h}$ is estimated to be 0.67. Similarly, the final $P_{c,s}$ for Run 3 is 0.98, and $P_{c,h}$ is estimated to be 0.53. These estimated values are slightly higher than the experimental values of $P_{c,h}$ of 0.60 in Run 2 and $P_{c,h}$of 0.45 in Run 3, but are generally in agreement. In the experiments, bars formed and the alluvial cover and sediment transport rate change spatially and temporally, resulting in a more complicated relationship than that expressed by equation (5). However, we conclude that in Runs 2 and 3 the erosion rates of the soft and hard bedrock are equal because the alluvial cover offsets difference in erodibility.

4.3 Bed roughness

According to Mishra and Inoue (2020), the alluvial cover fraction depends on bed roughness, flow discharge, bed slope, so the difference in alluvial cover on hard and soft bedrock areas is caused by the difference in bed roughness. The hydraulic roughness of mixed alluvial rivers is classified into skin friction from the unevenness of the bedrock surface k_{sb}^{surf}, form drag due to steps between hard and soft bedrock k_{sb}^{form}, surface drag due to the unevenness of the alluvial surface k_{sa}^{surf}, and form drag due to alluvial bedforms such as bars and dunes k_{sa}^{form}. In addition, Nelson and Seminara (2012) and Inoue et al. (2014) proposed that the total flow resistance is a linear combination of the flow resistance of the bedrock areas and the flow resistance of the alluvial areas, scaled by the alluvial cover fraction. Making this assumption, the roughness of the hard bedrock $k_{s,h}$ and the roughness of the soft bedrock $k_{s,s}$ can be expressed as follows,

$$k_{s,h} = \left(1 - P_{c,h}\right)\left(k_{sb,h}^{surf} + k_{sb}^{form}\right) + P_{c,h}\left(k_{sa}^{surf} + k_{sa}^{form}\right) \quad (6)$$

https://doi.org/10.5194/egusphere-2026-6373
Preprint. Discussion started: 19 November 2026
© Author(s) 2026. CC BY 4.0 License.

$$k_{s,s} = (1 - P_{c,s})(k_{sb,s}^{surf} + k_{sb}^{form}) + P_{c,s}(k_{sa}^{surf} + k_{sa}^{form}) \quad (7)$$

where, $k_{sb,h}^{surf}$ is the surface drag for hard bedrock and $k_{sb,s}^{surf}$ is the surface drag for soft bedrock.

Applying these equations requires values of at least some of the different k_s terms. k_{sa}^{surf} is generally 1 to 4 times grain size (e.g., Kamphius, 1974; Parker, 1991), and k_{sa}^{form} is known to be a function of the wave height and wavelength of alluvial bedforms (e.g. Grant and Madsen, 1982). The wavelength and wave height of bars formed on bedrock has been estimated by a two-dimensional numerical model (Inoue et al., 2016; Cho and Nelson, 2024a, b). Additionally, the wavelengths and wave heights of ripples, dunes, and antidunes formed on partially deposited sediments can be predicted using theoretical models (e.g., Engelund, 1970; Colombini, 2004; Andreotti et al., 2012; Inoue et al., 2020), and numerical models (e.g. Giri and Shimizu, 2006; Bohorquez and Ancey, 2016; Doré et al., 2016; Olsen, 2017). However, it is far less clear what controls k_{sb}^{surf} and k_{sb}^{form}. For example, why are the standard deviations of soft bedrock surface roughness different between Run 2 and Run 3, even though the soft rock strength is the same? Why is step height the same in Runs 2 and 3, even though the hard rock strength is different? Bedrock surface and form drag may depend not only on the bedrock strength, but also on interactions between bedrock erosion, development of surface roughness, and the impact of the changing topography on near-bed hydraulics and sediment transport. Similar to controls on the surface and form drag of alluvial beds, these processes will depend on factors such as the grain size of the overpassing sediment, the channel aspect ratio, and the Froude and Reynolds numbers. A more detailed understanding of k_{sb}^{surf} and k_{sb}^{form} will be an interesting future challenge, as it will enable more accurate predictions of alluvial cover and water depth in bedrock rivers.

5 Conclusions

In this study, we investigated changes in bedrock erosional topography, hydraulic roughness, bedrock surface irregularity, and alluvial cover using a flume in which bedrock strength changes at regular intervals downstream. Under small differences in rock strength, longitudinal grooves, were formed by turbulence-driven secondary flows, and there was very little difference in the elevation of soft and hard bedrock areas. When the difference in rock strength was larger, alluvial alternate bars formed on the bedrock, and bedrock steps formed at the boundaries between the soft and hard bedrock. In the early stage of the experiments with bedrock steps, the bedrock step height increased over time, but the step height growth rate gradually slowed down and the bed eventually converged to a constant step height. This suggests that dynamic equilibrium was reached, with equal erosion rates of hard and soft bedrocks. We hypothesize that the erosion rates were the same, despite the difference in rock strength, because of the difference in the alluvial cover fraction. The cover fraction on the soft bedrock was larger than that on the hard bedrock, which equalized the erosion rates. When the difference in rock strength was further increased in Run 3, the step height didn't change due to the adjustment of the alluvial cover fraction.

https://doi.org/10.5194/egusphere-2026-6373
Preprint. Discussion started: 19 November 2026
© Author(s) 2026. CC BY 4.0 License.

Code and data availability

All experimental data is provided in the Supporting Information and repository,
https://doi.org/10.5281/zenodo.19351981

Author contributions

Kazuaki Mutsuura ; Methodology, Writing - Original Draft, Formal analysis, Investigation, Data Curation. Takuya Inoue; Conceptualization, Formal analysis, Supervision. Tamaki Sumner; Investigation, Data Curation, Visualization, carried them out. Rebecca Hodge; Writing - Review & Editing. and Tatsuhiko Uchida; Writing - Review & Editing.

Disclaimer

Copernicus Publications remains neutral with regard to jurisdictional claims made in the text, published maps, institutional affiliations, or any other geographical representation in this paper. While Copernicus Publications makes every effort to include appropriate place names, the final responsibility lies with the authors. Views expressed in the text are those of the authors and do not necessarily reflect the views of the publisher.

Acknowledgements

We acknowledge support from JSPS KAKENHI Grant Number 23K22872 and 22KK0239.

References

Andreotti, B., Claudin, P., Devauchelle, O., Durán, O., and Fourrière, A.: Bedforms in a turbulent stream: ripples, chevrons and antidunes, Journal of Fluid Mechanics 690: 94–128. https://doi.org/10.1017/jfm.2011.386, 2012.

Aubert, G., Langlois, V. J., and Allemand, P.: Bedrock incision by bedload: insights from direct numerical simulations, Earth Surf. Dynam., 4, 327–342, https://doi.org/10.5194/esurf-4-327-2016, 2016.

Auel, C., Boes, R. M., and Sumi, T.: Sediment bypass tunnel design – review and outlook, J. Hydraul. Eng., 141, 12, https://doi.org/10.1061/(ASCE)HY.1943-7900.0001053, 2015.

Baynes, E. R. C., Lague, D., Steer, P., Bonnet, P., and Illien, L.: Sediment flux-driven channel geometry adjustment of bedrock and mixed gravel–bedrock rivers, Earth Surf. Process. Landforms, 45: 3714–3731. https://doi.org/10.1002/esp.4996, 2020.

Bohorquez P, Ancey C. : Particle diffusion in non-equilibrium bedload transport simulations, Applied Mathematical Modelling 40: 7474–7492. https://doi.org/10.1016/j.apm.2016.03.044, 2016.

https://doi.org/10.5194/egusphere-2026-6373
Preprint. Discussion started: 19 November 2026
© Author(s) 2026. CC BY 4.0 License.



Chatanantavet, P., and Parker, G.: Experimental study of bedrock channel alleviation under varied sediment supply and hydraulic conditions, Water Resour. Res., 44, W12446, https://doi.org/10.1029/2007WR006581, 2008.

Chatanantavet, P., & Parker, G.: Physically based modeling of bedrock incision by abrasion, plucking, and macroabrasion, Journal of Geophysical Research, Earth Surface, 114(F4), https://doi.org/10.1029/2008JF001044, 2009.

Cho, J., & Nelson, P. A.: Patterns of alluviation in mixed bedrock-alluvial channels: 1. Numerical model, Journal of Geophysical Research: Earth Surface, 129, e2023JF007292. https://doi.org/10.1029/2023JF007292, 2024a.

Cho, J., & Nelson, P. A.: Patterns of alluviation in mixed bedrock-alluvial channels: 2. controls on the formation of alluvial patches, Journal of Geophysical Research: Earth Surface, 129, e2023JF007293. https://doi.org/10.1029/2023JF007293, 2024b.

Colombini, M.: Revisiting the linear theory of sand dune formation. Journal of Fluid Mechanics 502: 1–16. https://doi.org/10.1017/S0022112003007201, 2004.

Colombini, M., Seminara, G., & Tubino, M.: Finite-amplitude alternate bars, Journal of Fluid Mechanics, 181(-1), 213–232. https://doi.org/10.1017/S0022112087002064, 1987.

Doré A, Bonneton P, Marieu V, Garlan T.: Numerical modeling of subaqueous sand dune morphodynamics. Journal of Geophysical Research - Earth Surface 121: 565–587. https://doi.org/10.1002/2015JF003689, 2016.

Engelund F.: Instability of erodible beds. Journal of Fluid Mechanics 42: 225–244, https://doi.org/10.1017/S0022112070001210, 1970.

Fernández, R., Parker, G., Roberto, F., Stark, C. P.: Experiments on patterns of alluvial cover and bedrock erosion in a meandering channel, Earth Surf. Dynam., 7, 949–968, https://doi.org/10.5194/esurf-7-949-2019, 2019.

Gilbert, G. K.: Report on the Geology of the Henry Mountains: Geographical and Geological Survey of the Rocky Mountain Region, 160 pp., U.S. Gov. Print. Off., Washington, D. C., https://doi.org/10.5962/bhl.title.51652, 1877.

Giri S, Shimizu Y.: Numerical computation of sand dune migration with free surface flow, Water Resources Research 42: W10422. https://doi.org/10.1029/2005WR004588, 2006.

Grant, W. D., & Madsen, O. S.: Movable bed roughness in unsteady oscillatory flow, Journal of Geophysical Research, 87(C1), 469–481. https://doi.org/10.1029/JC087iC01p00469, 1982.

Hodge, R. A., and T. B. Hoey.: Upscaling from grain-scale processes to alluviation in bedrock channels using a cellular automaton model, J. Geophys. Res., 117, F01017, https://doi.org/10.1029/2011JF002145, 2012.

Hodge, R. A., and T. B. Hoey.: A Froude-scaled model of a bedrock-alluvial channel reach: 1. Hydraulics, J. Geophys. Res. Earth Surf., 121, 1578–1596, https://doi.org/10.1002/2015JF003706, 2016a.

Hodge, R. A., and T. B. Hoey.: A Froude-scaled model of a bedrock-alluvial channel reach: 2. Sediment cover, J. Geophys. Res. Earth Surf., 121, 1597–1618, https://doi.org/10.1002/2015JF003709, 2016b.

Hubert, C.: Hydraulics of Skimming Flows over Stepped Spillways: Journal of Hydraulic Research, Vol. 32, No. 3, pp. 445-458, https://doi.org/10.1080/00221689409498745, 1994.

Inoue, T., Hiramatsu, Y., Scheingross, J. S., Yamaguchi, S., & Takahashi, K.: Controls on erosion and cyclic step-formation upstream of waterfalls, Geophysical Research Letters, 51, e2024GL110751. https://doi.org/10.1029/2024GL110751, 2024.

https://doi.org/10.5194/egusphere-2026-6373
Preprint. Discussion started: 19 November 2026
© Author(s) 2026. CC BY 4.0 License.



Inoue, T., Izumi, N., Scheingross, J.S., Hiramatsu, Y., Tanigawa, S., & Sumner, T.: Waterfall height sets the mechanism and rate of upstream retreat, Geology, 51(7), 693–697. https://doi.org/10.1130/G51039.1, 2023.

Inoue, T., Izumi, N., Shimizu, Y., & Parker, G.: Interaction among alluvial cover, bed roughness, and incision rate in purely bedrock and alluvial-bedrock channel, Journal of Geophysical Research: Earth Surface, 119, 2123–2146. https://doi.org/10.1002/2014JF003133, 2014.

Inoue, T., Iwasaki, T., Parker, G., Shimizu, Y., Izumi, N., Stark, C. P., & Funaki, J.: Numerical simulation of effects of sediment supply on bedrock channel morphology, Journal of Hydraulic Engineering, 142(7), 04016014. https://doi.org/10.1061/(ASCE)HY.1943-7900.0001124, 2016.

Inoue, T., Mishra, J., & Parker, G.: Numerical simulations of meanders migrating laterally as they incise into bedrock, Journal of Geophysical Research: Earth Surface, 126, e2020JF005645. https://doi.org/10.1029/2020JF005645, 2021.

Inoue, T., & Nelson, J. M.: An experimental study of longitudinal incisional grooves in a mixed bedrock-alluvial channel, Water Resources Research, 56, e2019WR025410. https://doi.org/10.1029/2019WR025410, 2020.

Inoue, T., Yamaguchi, S., and Nelson, J. M.: The effect of wet-dry weathering on the rate of bedrock river channel erosion by saltating gravel, Geomorphology, 285(15), 152–161. https://doi.org/10.1016/j.geomorph.2017.02.0, 2017.

Inoue, T., Watanabe, Y., Iwasaki, T., and Otsuka, J.: Three-dimensional antidunes coexisting with alternate bars, Earth Surf. Process. Landforms, 45: 2897–2911. https://doi.org/10.1002/esp.4938, 2020.

Johnson, J. P.: A surface roughness model for predicting alluvial cover and bedload transport rate in bedrock channels, J. Geophys. Res. Earth Surface, https://doi.org/10.1002/2013JF003000, 2014.

Johnson, J. P. L., and K. X. Whipple.: Evaluating the controls of shear stress, sediment supply, alluvial cover, and channel morphology on experimental bedrock incision rate, J. Geophys. Res., 115, F02018, https://doi.org/10.1029/2009JF001335, 2010.

Kamphius, J. W.: Determination of sand roughness for fixed beds, J. Hydraul. Res., 12(2), 193–203, https://doi.org/10.1080/00221687409499737, 1974.

Kuroki, M., & Kishi, T.: Regime criteria on bars and braids in alluvial straight channels, Proceedings of the Japan Society for Comparative Endocrinology, 342, 87–96. (in Japanese). https://doi.org/10.2208/jscej1969.1984.342_87, 1984.

Mishra, J. and Inoue, T.: Alluvial Cover on Bedrock Channel: Applicability of Existing Models, Earth Surface Dynamics, 8, pp.695–716, https://doi.org/10.1029/2011GL050806, 2020.

Nelson, P. A., and G. Seminara.: A theoretical framework for the morphodynamics of bedrock channels, Geophys. Res. Lett., 39, L06408, https://doi.org/10.1029/2011GL050806, 2012.

Olsen NRB.: Numerical modelling of downstream-migrating antidunes, Earth Surface Processes and Landforms 42: 2393–2401, https://doi.org/10.1002/esp.4193, 2017.

Parker, G.: Selective sorting and abrasion of river gravel, 1: Theory, J. Hydraul. Eng., 117(2), 131–149, https://doi.org/10.1061/(ASCE)0733-9429(1991)117:2(131), 1991.

https://doi.org/10.5194/egusphere-2026-6373
Preprint. Discussion started: 19 November 2026
© Author(s) 2026. CC BY 4.0 License.



Shobe, C. M., Tucker, G. E., and Barnhart, K. R.: The SPACE 1.0 model: a Landlab component for 2-D calculation of sediment transport, bedrock erosion, and landscape evolution, Geosci. Model Dev., 10, 4577–4604, https://doi.org/10.5194/gmd-10-4577-2017, 2017.

Sklar, L. S., and W. E. Dietrich.: River longitudinal profiles and bedrock incision models: Stream power and the influence of sediment supply, in Rivers Over Rock: Fluvial Processes in Bedrock Channels, Geophys. Monogr. Ser., vol. 107, edited by K. Tinkler and E. E. Wohl, pp. 237–260, AGU, Washington, D. C., https://doi.org/10.1029/GM107p0237, 1998.

Sklar, L. S., & Dietrich, W. E.: A mechanistic model for river incision into bedrock by saltating bed load, Water Resources Research, 40, W06301. https://doi.org/10.1029/2003WR002496, 2004.

Turowski, J. M., D. Lague, and N. Hovius.: Cover effect in bedrock abrasion: A new derivation and its implications for the modeling of bedrock channel morphology, J. Geophys. Res., 112, F04006, doi:10.1029/2006JF000697, 2007.

Zhang, L., Parker, G., Stark, C. P., Inoue, T., Viparelli, E., Fu, X., and Izumi, N.: Macro-roughness model of bedrock–alluvial river morphodynamics, Earth Surf. Dynam., 3, 113–138, https://doi.org/10.5194/esurf-3-113-2015, 2015.